

321 A Extensions

322 We explore additional extensions of GloptiNets that further enhance its appeal. We first describe
 323 a block diagonal structure for the model for faster evaluation, a theoretical splitting scheme for
 324 optimization, and finally a warm start scheme.

325 A.1 Block diagonal structure for efficient computation

326 Without any further assumption, we see that a model from definition [1](#) can be evaluated in $O(rmd)$
 327 time; its Fourier coefficient given by lemma [1](#) in $O(m^2d)$; the bound on the RKHS norm is computed
 328 in $O(m^3d)$ time thanks to lemma [2](#); all that enables to compute a certificate, as stated in theorem [2](#),
 329 in $O(N(m^2d) + m^3)$ time, where N is the number of frequencies sampled. If the function f to be
 330 minimized has big \mathcal{H}_s norm, we might need a large model size m to have $f - f_* \approx g$. Hence, we
 331 introduce specific structure on G which makes it *block-diagonal* and *better conditioned*, so that the
 332 complexity on m and the positivity constraint are alleviated.

333 **Proposition 2** (Block-diagonal PSD model). *Let g be a PSD model as in definition [1](#) with $m = bs$
 334 anchors. Split them into b groups, denoting them \mathbf{z}_{ij} , $i \in [b]$ and $j \in [s]$. Compute the Cholesky
 335 factorization of each kernel matrix $T_i^\top T_i = K_{\mathbf{z}_i} \in \mathbb{R}^{s \times s}$. Then, define G as a block-diagonal matrix,
 336 with b blocks defined as $G_i = \tilde{R}_i \tilde{R}_i^\top$, $\tilde{R}_i = T^{-1} R_i$, and $R_i \in \mathbb{R}^{r \times s}$. Equivalently,*

$$G = \begin{pmatrix} \tilde{R}_1 \tilde{R}_1^\top & & \\ & \ddots & \\ & & \tilde{R}_b \tilde{R}_b^\top \end{pmatrix}, \quad \text{s.t. } g(x) = \sum_{i=1}^b \|R_i^\top K_{\mathbf{z}_i}(x)\|^2, \quad K_{\mathbf{z}_i}(x) = K(\mathbf{z}_{ij}, x)_{1 \leq j \leq s}. \quad (21)$$

337 Then g can be evaluated in $O(rbs^3d)$ time, \hat{g}_ω in $O(bs^2(r+d+s))$ time, and $\|g\|_{\mathcal{S}(\mathcal{H}_s)}^2$ in $O(b^2(rs^2 +$
 338 $r^2s) + bs^3)$ time. The model has $(r+d)bs$ real parameters.

339 *Proof.* Having G defined as such, it is psd, of rank at most $rb \leq sb = m$. Written $g(x) =$
 340 $\sum_{i=1}^b \|R_i^\top K_{\mathbf{z}_i}(x)\|^2$, we can compute the Fourier coefficient by applying lemma [1](#) to each of the b
 341 component. Adding the cost of computing $G_i = \tilde{R}_i \tilde{R}_i^\top$ results in complexity of $O(bs^2(r+d+s))$.
 342 Finally, note that $\|g\|_{\mathcal{S}(\mathcal{H}_s)}^2 = \|A\|_{\mathcal{S}(\mathcal{H}_s)}^2$ where

$$A = ((\varphi(\mathbf{z}_{1j}))_{j \in [s]}, \dots, (\varphi(\mathbf{z}_{bj}))_{j \in [s]})(\text{Diag } G_i)_{i \in [b]}((\varphi(\mathbf{z}_{1j}))_{j \in [s]}, \dots, (\varphi(\mathbf{z}_{bj}))_{j \in [s]})^*.$$

343 Then, defining Q the matrix of $b \times b$ blocks of size $s \times s$ s.t. for $j, k \in [b]$, $Q_{jk} = K(\mathbf{z}_j, \mathbf{z}_k) \in \mathbb{R}^{s \times s}$,
 344 we have

$$\|A\|_{\mathcal{S}(\mathcal{H}_s)}^2 = \text{Tr } Q(\text{Diag } G_i)_{i \in [b]} Q(\text{Diag } G_i)_{i \in [b]} = \sum_{j,k=1}^b \text{Tr } G_j Q_{jk} G_k Q_{kj}, \quad (22)$$

345 and each term in the sum can be written $\text{Tr}(\tilde{R}_j^\top Q_{jk} \tilde{R}_k)(\tilde{R}_k^\top Q_{kj} \tilde{R}_j^\top) = \|\tilde{R}_j^\top Q_{jk} \tilde{R}_k\|_{HS}^2$, which is
 346 computed in $O(s^2r + sr^2)$ time, plus $O(bs^3)$ to compute the Cholesky factor. \square

347 Denoting $\varphi_{\mathbf{z}_i} = (\varphi(\mathbf{z}_{ij}))_{1 \leq j \leq s}$, note that

$$\varphi_{\mathbf{z}_i} G_i \varphi_{\mathbf{z}_i}^* = \varphi_{\mathbf{z}_i} T_i^{-1} R_i R_i^\top (\varphi_{\mathbf{z}_i} T_i^{-1})^* = E_i R_i R_i^\top E_i^*, \quad (23)$$

348 with $E_i = \varphi_{\mathbf{z}_i} T_i^{-1}$ an orthonormal basis of $\text{Span}(\varphi_{\mathbf{z}_i})_{1 \leq i \leq b}$ as $E_i^* E_i = \mathbf{I}_s$. Thus, each model's
 349 coefficient is defined on an orthonormal basis, which makes the optimization easier.

350 **Remark 3** (Relation to Term Sparsity in POP). *The successful application of polynomial hierarchies
 351 to problems with thousands of variables rely on making the moment matrix M having a block
 352 structure [\[11\]](#) [\[12\]](#). If the monomial basis has size m , the constraint $M \succeq 0$ is replaced with
 353 $M = (\text{Diag } M_i)_{i \in [b]}$ and $M_i \succeq 0$. This enables to solve b SDP of size at most s instead of one of
 354 size m . Our model in proposition [2](#) follows a similar route for having a lower computational budget.*

355 A.2 Global optimization with splitting scheme

356 While GloptiNets can provide certificates for functions, it falls behind local solvers in terms of
 357 competitiveness. The challenge lies in the fact that finding a certificate is considerably more dif-
 358 ficult than locating a local minimum, as it necessitates the uniform approximation of the entire
 359 function. However, we present a novel algorithmic framework that has the potential to enhance the
 360 competitiveness of GloptiNets with local solvers while simultaneously delivering certificates. Our
 361 approach involves partitioning the search domain into multiple regions and computing lower bounds
 362 for each partition. By discarding portions of the domain where the lower bound exceeds a certain
 363 threshold, the algorithm progressively simplifies the optimization problem and removes areas from
 364 consideration. Moreover, such an approach is naturally well suited to parallel computation.

365 The algorithm relies on a divide-and-conquer mechanism. First, we split the hypercube $(-1, 1)^d$ in
 366 N regions, where N is the number of core available. We compute an upper bound with a local solver.
 367 For each region, we run GloptiNets *in parallel*, computing a certificate at regular interval. As soon as
 368 the certificate is bigger than the upper bound, we stop the process: we know that the global minimum
 369 is not in the associated region. We can then reallocate the freed computing power by splitting the
 370 biggest current region, which yields an easier problem. We stop as soon as the region considered are
 371 small enough. This is summarized in alg. 2, where \textcircled{P} indicates the loop run in parallel.

372 Note that minimizing f on a hypercube of center μ and size σ amounts to minimizing $x \mapsto f((x -$
 373 $\mu)/\sigma)$ on $[-1, 1]^d$, which is another Chebychev polynomial whose coefficients can be evaluated
 374 efficiently thanks to the order-2 relation every orthonormal polynomial satisfy. For Chebychev
 375 polynomials, that is $H_{\omega+1}(x) = 2xH_{\omega}(x) - H_{\omega-1}(x)$.

Algorithm 2: Splitting scheme with GloptiNets

Data: A Chebychev polynomial f with a unique global optimum, a probability δ , a number of
 cores N and a volume $\rho < 1/N$.

Result: A certificate on f : $f_{\star} \geq C_{\delta}(f)$ with proba. $1 - \delta_{\star}$.

/* Initialization: upper bound and partition */

$\Pi = \text{partition}([-1, 1]^d, N), \delta_{\star} = 0$;

\textcircled{P} $\text{ub} = \min_{\pi \in \Pi} \{\text{localsolver}_{x \in \pi} f(x)\}$;

/* Iterate over the partition */

\textcircled{P} **for** $\pi \in \Pi$, **While** $\text{length}(\Pi) > 1$ **do**

while $C_{\delta}(f_{\pi}) < \text{ub}$ **do**

 | Continue optimization;

 Split biggest part: $\pi_0 = \arg \max_{\pi \in \Pi} \text{Vol}(\pi)$; $(\pi_1, \pi_2) = \text{partition}(\pi_0, 2)$;

 If $\text{Vol}(\pi_{1,2}) < \rho$: end this process ;

 Update upper bound: $\text{ub} = \min \{\text{ub}, \text{localsolver}_{x \in \pi_{1,2}} f(x)\}$;

 Update search space and δ_{\star} : $\Pi = \Pi \setminus \{\pi, \pi_0\} \cup \{\pi_1, \pi_2\}$, $\delta_{\star} = 1 - (1 - \delta_{\star})(1 - \delta)$;

/* A single region in Π remains */

Returns $\Pi = \{\pi\}, C_{\delta}(f_{\pi}), \delta_{\star}$;

376 A.3 Warm restarts

377 Our model distinguishes itself by leveraging the analytical properties of the objective function,
 378 rather than relying solely on algebraic characteristics. This approach offers a notable advantage,
 379 as closely related functions can naturally benefit from a warm restart. For example, if we already
 380 have a certificate for a function f using a PSD model g , and we seek to compute a certificate for
 381 a similar function $\tilde{f} \approx f$, we can readily employ GloptiNets by initializing the PSD model with g .
 382 In contrast, P-SoS methods, which rely on SDP programs, cannot directly adapt to new problems
 383 without significant effort. For instance, if a new component is introduced, an entirely new SDP must
 384 be solved. Our model’s ability to accommodate related yet distinct problems could prove highly
 385 valuable in domains with a frequent need to certify different but closely related problems. In the
 386 industry, the Optimal Power Flow (OPF) problem requires periodic solves every 5 minutes [21].
 387 With GloptiNets, once the initial challenging solve is performed, subsequent solves become easier
 388 assuming minimal changes in supply and demand conditions.

389 B Kernel defined on the Chebychev basis

390 In this section we describe the approach we take to model functions written in the Chebychev basis.
 391 For f such a polynomial, a naive approach would simply model $\tilde{f} = f \circ \cos(2\pi \cdot)$ as a trigonometric
 392 polynomial. However, note that the decomposition of \tilde{f} only has cosine terms. Thus, approximating
 393 $f - f_*$ efficiently requires a PSD model which has only cosine terms in its Fourier decomposition.
 394 This is achieved by using a kernel written in the Chebychev basis, as introduced in proposition 1, for
 395 which we now provide a proof.

396 *Proof of proposition 1* Let $x, y \in [-1, 1]$ and $u, v \in [0, 1/2]$ s.t. $x, y = \cos(2\pi u), \cos(2\pi v)$, by
 397 bijectivity of the cosine function on $[0, \pi]$. From the definition of K in eq. (19) and the definition of q
 398 in eq. (5), we have that

$$\begin{aligned} K(x, y) &= \frac{1}{2} \sum_{\omega \in \mathbb{Z}} \hat{q}_\omega \left(e^{2\pi i \omega (u+v)} + e^{2\pi i \omega (u-v)} \right) \\ &= \sum_{\omega \in \mathbb{Z}} \hat{q}_\omega e^{2\pi i \omega u} \cos(2\pi \omega v) \\ &= \hat{q}_0 + 2 \sum_{\omega \in \mathbb{N}} \hat{q}_\omega \cos(2\pi \omega u) \cos(2\pi \omega v) \\ &= \hat{q}_0 + 2 \sum_{\omega \in \mathbb{N}} \hat{q}_\omega H_\omega(u) H_\omega(v). \end{aligned}$$

399 Since q has positive Fourier transform, this makes the feature map of K explicit with $K(x, y) =$
 400 $\varphi(u) \cdot \varphi(v)$, $\varphi(u)_\omega = \sqrt{(1 + \mathbf{1}_{\omega \neq 0}) \hat{q}_\omega} H_\omega(u)$, for $\omega \in \mathbb{N}$. Hence the kernel is a reproducing
 401 kernel. \square

402 We now use this kernel with the Bessel function $x \mapsto e^{s(\cos(2\pi x) - 1)}$, i.e. we define the kernel K on
 403 $[-1, 1]$ to satisfy

$$\forall u, v \in (0, 1/2), \quad K(\cos(2\pi u), \cos(2\pi v)) = \frac{1}{2} \left(e^{s(\cos(2\pi(u+v)) - 1)} + e^{s(\cos(2\pi(u-v)) - 1)} \right). \quad (24)$$

404 As it was the case for the torus, this kernel enables an easy characterization of a RKHS in which an
 405 associated PSD model g lives.

406 **Lemma 3** (Chebychev coefficient of the Bessel kernel). *Let g be a PSD model as in definition 1 with*
 407 *the kernel K of eq. (24). Then, the Chebychev coefficient $\omega \in \mathbb{N}^d$ of g can be computed in $O(m^2 d)$*
 408 *time with*

$$g_\omega = \sum_{i,j=1}^m A_{ij} \prod_{\ell=1}^d (1 + \mathbf{1}_{\omega \neq 0}) \frac{e^{-2s_\ell}}{2} \left[\begin{aligned} &I_{\omega_\ell}(2s_\ell \sigma_{-\ell ij}) H_{\omega_\ell}(\sigma_{+\ell ij}) \\ &+ I_{\omega_\ell}(2s_\ell \sigma_{+\ell ij}) H_{\omega_\ell}(\sigma_{-\ell ij}) \end{aligned} \right] \quad (25)$$

409 where

$$\sigma_{\pm \ell ij} = \cos(2\pi m_{\pm \ell ij}), \quad m_{\pm \ell ij} = (\mathbf{u}_{\ell ij} \pm \mathbf{u}_{\ell ij})/2, \quad \text{and} \quad \cos 2\pi \mathbf{u}_{\ell ij} = \mathbf{z}_{\ell ij}.$$

410 *Proof.*

411 **Expanding g and definition of Chebychev coefficient.** From the definition of g in eq. (4), we have

$$g(\mathbf{x}) = \sum_{i,j=1}^m A_{ij} \prod_{\ell=1}^d K_{s_\ell}(\mathbf{x}_\ell, \mathbf{z}_{\ell i}) K_{s_\ell}(\mathbf{x}_\ell, \mathbf{z}_{\ell j}). \quad (26)$$

412 We consider $x, y, z \in (-1, 1)$ and $s > 0$. We denote $u, v, w \in (0, 1/2)$ s.t.

$$x, y, z = \cos 2\pi u, \cos 2\pi v, \cos 2\pi w$$

413 with the bijectivity of $x \mapsto \cos(2\pi x)$ on $(0, 1/2)$. We now compute the Chebychev coefficient of
 414 $x \mapsto K_s(x, y)K_s(x, z)$. Denoted h_ω , this is

$$\forall \omega \in \mathbb{N}, h_\omega = \frac{1 + \mathbf{1}_{\omega \neq 0}}{\pi} \int_{-1}^1 K_s(x, y)K_s(x, z)T_\omega(x) \frac{dx}{\sqrt{1-x^2}},$$

415 or equivalently

$$\forall \omega \in \mathbb{N}, h_\omega = (1 + \mathbf{1}_{\omega \neq 0}) \int_0^1 K_s(\cos 2\pi u, \cos 2\pi v)K_s(\cos 2\pi u, \cos 2\pi w) \cos(2\pi \omega u) du. \quad (27)$$

416

417 **Chebychev coefficient of kernel product.** With the definition of the kernel in proposition [1](#)
 418 eq. [\(19\)](#), we have

$$\begin{aligned} K_s(x, y)K_s(x, z) &= \frac{1}{4} (h(u+v) + h(u-v)) \times (h(u+w) + h(u-w)) \\ &= \frac{e^{-2s}}{4} \left(e^{s \cos 2\pi(u+v)} + e^{s \cos 2\pi(u-v)} \right) \times \left(e^{s \cos 2\pi(u+w)} + e^{s \cos 2\pi(u-w)} \right) \end{aligned}$$

419 Now use the sum-to-product formula with the cosines to obtain

$$K_s(x, y)K_s(x, z) = \frac{e^{-2s}}{4} \left(e^{2s \cos 2\pi(\frac{v-w}{2}) \cos 2\pi(u+\frac{v+w}{2})} + e^{2s \cos 2\pi(\frac{v-w}{2}) \cos 2\pi(u-\frac{v+w}{2})} \right. \\ \left. + e^{2s \cos 2\pi(\frac{v+w}{2}) \cos 2\pi(u+\frac{v-w}{2})} + e^{2s \cos 2\pi(\frac{v+w}{2}) \cos 2\pi(u-\frac{v-w}{2})} \right), \quad (28)$$

420 We simplify this expression by introducing

$$m_\pm = \frac{1}{2}(v \pm w) \text{ and } \sigma_\pm = \cos 2\pi m_\pm. \quad (29)$$

421 Then, eq. [\(28\)](#) becomes

$$K_s(x, y)K_s(x, z) = \frac{e^{-2s}}{4} \left(e^{2s\sigma_- \cos 2\pi(u+m_+)} + e^{2s\sigma_- \cos 2\pi(u-m_+)} \right. \\ \left. + e^{2s\sigma_+ \cos 2\pi(u+m_-)} + e^{2s\sigma_+ \cos 2\pi(u-m_-)} \right). \quad (30)$$

422 We recognize the definition of the kernel (which is not a surprise as we chose the kernel to be stable
 423 by product). However, we need variables in $(0, 1/2)$ to retrieve the proper definition of the kernel.
 424 Instead, we use lemma [4](#) on eq. [\(30\)](#) combined with eq. [\(27\)](#), to obtain

$$h_\omega = (1 + \mathbf{1}_{\omega \neq 0}) \frac{e^{-2s}}{4} \left(\cos(2\pi \omega m_+) I_\omega(2s\sigma_-) + \cos(2\pi \omega m_+) I_\omega(2s\sigma_-) \right. \\ \left. + \cos(2\pi \omega m_-) I_\omega(2s\sigma_+) + \cos(2\pi \omega m_-) I_\omega(2s\sigma_+) \right),$$

425 which gives

$$h_\omega = (1 + \mathbf{1}_{\omega \neq 0}) \frac{e^{-2s}}{2} (\cos(2\pi \omega m_+) I_\omega(2s\sigma_-) + \cos(2\pi \omega m_-) I_\omega(2s\sigma_+)). \quad (31)$$

426 Equation [\(31\)](#) contains the Chebychev coefficient of the product of two kernel function as defined
 427 in eq. [\(27\)](#). Plugging this result into the definition of g in eq. [\(26\)](#), and noting that $\cos(2\pi \omega m_\pm) =$
 428 $H_\omega(\cos 2\pi m_\pm) = H_\omega(\sigma_\pm)$, we obtain the result. \square

429 Thanks to lemma [3](#), we see that a model g defined as in definition [1](#) with the Bessel kernel K_s of
 430 eq. [\(24\)](#) as its Chebychev coefficients decaying in $O(I_\omega(2s))$. Hence, it belongs to \mathcal{H}_{2s} , the RKHS
 431 associated to K_{2s} .

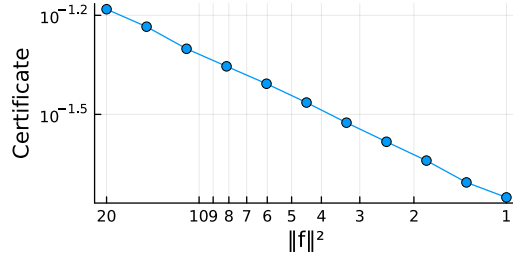


Figure 3: Certificate vs. RKHS norm of f , for a given model g with a fixed number of parameters. f has 1146 coefficients and g has 22528 parameters. Best certificate is kept among a set of optimization hyperparameters. As the norm of f decreases, fitting $f - f_*$ with g is easier and the certificate becomes tighter.

432 C Additional details on the experiments

433 **Regularization.** Regularization is performed by approximating the HS norm with a proxy which
 434 is faster to compute. We use $\|R_j^\top \hat{R}_k\|_{HS}^2$ instead of $\|\hat{R}_j^\top Q_{jk} \hat{R}_k\|_{HS}^2$ in eq. (22).

435 **Hardware.** GloptiNets was used with NVIDIA V100 GPUs for the interpolation part, and Intel
 436 Xeon CPU E5-2698 v4 @ 2.20GHz for computing the certificate. TSSOS was ran on a Apple M1
 437 chip with Mosek solver.

438 **Configuration of TSSOS.** We use the lowest possible relaxation order d (i.e. $\lceil \deg f / 2 \rceil$), along
 439 with Chordal sparsity. We use the first relaxation step of the hierarchy. In these settings, TSSOS is
 440 not guaranteed to converge to f_* but will executes the fastest.

441 **Certificate vs. number of parameter for a given function.** In fig. 2, the target function is a
 442 random polynomial of norm 1. The models forming the blue line are defined as in proposition 2 with
 443 rank, block size and number of blocks equal to $(1, bs, 1)$ respectively, with bs the block size we vary.
 444 The number of frequencies sampled to compute the certificate is 160000, and accounts for the fact
 445 that the bound on the variance becomes larger than the MOM estimator for large models.

446 **Certificate vs. problem difficulty for a given model.** We have 3 related parameters: the quality
 447 of the optimization (given by the certificate), the expressivity of the model (given by its number of
 448 parameters), and the difficulty of the optimization (given by the norm of the function). In fig. 2 we
 449 fix the latter and plot the relation between the first two. Here, we fix the model with parameters
 450 $(8, 16, 128)$, and we optimize a polynomial in $3d$ of degree 12, with RKHS norm ranging from 1 to
 451 20. The certificates obtained are given in fig. 3. The resulting plot exhibits a clear polynomial relation
 452 between the certificate and the norm of the function, with a slope of -0.88 . This suggest that the
 453 certificate behaves as $O(\|f\|_{\mathcal{H}_{2s}}^{-1})$.

454 **Comparison with TSSOS on the Fourier basis.** In table 1, the polynomials f all have a RKHS
 455 norm of 1. The small model is defined as in proposition 2 with rank, block size and number of blocks
 456 equal to 4, 8, 16 respectively. For the big models, those values are 8, 16, 32. The certificate is the
 457 maximum of the Chebychev bound of theorem 2 and the MoM bound of theorem 3. The number of
 458 frequencies sampled is 160000.

459 **Comparison with TSSOS on the Chebychev basis.** We compare GloptiNets with TSSOS on ran-
 460 dom Chebychev polynomials in table 2, similarly to the comparison with trigonometric polynomials
 461 in table 1. Minimizing polynomials defined on the canonical basis is easier: contrary to trigonometric
 462 polynomials, there is no need to account for the imaginary part of the variable. If d is the dimension,
 463 complex polynomials are encoded in a variable of dimension $2d$ in TSSOS, following the definition
 464 of Hermitian Sum-of-Squares introduced in [30]. Hence, the random polynomials we consider are
 465 characterized by the dimension d and their number of coefficients n ; instead of bounding the degree,
 466 we use all the basis elements $H_\omega(\mathbf{x}) = \prod_{\ell=1}^d H_{\omega_\ell}(x_\ell)$ for which $\|\omega\|_\infty \leq p$. The maximum degree

Table 2: GloptiNets and TSSOS on random Chebychev polynomials. The same conclusion as in table 1 applies. While TSSOS is very efficient on small problems, its memory requirements grow exponentially with the problem size. GloptiNets has less accuracy, but a computational burden which does not increase with the problem size.

d	p	n	TSSOS		GN-small		GN-big	
			Certif.	t	Certif.	t	Certif.	t
	3	255	$3.4 \cdot 10^{-7}$	6	$9.3 \cdot 10^{-2}$	54	$3.3 \cdot 10^{-2}$	264
	4	624	$2.1 \cdot 10^{-9}$	153	$8.3 \cdot 10^{-2}$	55	$2.8 \cdot 10^{-2}$	258
		5	Out of memory!	-	$1.0 \cdot 10^{-1}$	56	$3.2 \cdot 10^{-2}$	264

is then dp . The RKHS norm of f is fixed to 1. As with the comparison on Trigonometric polynomial table 1, we see that GloptiNets provides similar certificates no matter the number of coefficients in f . Even though it lags behind TSSOS for small polynomials, it handles large polynomials which are intractable to TSSOS. The “small” and “big” models have the same structure as for the trigonometric polynomials experiments.

Sampling from the Bessel distribution. The function $\omega \mapsto e^{-s}I_\omega(s)$ decays rapidly. In fact, with $s = 2$, which is the value used to generate the random polynomials, it falls under machine precision as soon as $\omega > 14$. Thus, we approximate the distribution with a discrete one with weights $I_\omega(s)$ for ω s.t. the result is above the machine precision. We then extend it to multiple dimension with a tensor product. Finally, we use a hash table to store the already sampled frequency, to make the evaluation of million of frequencies much faster. For instance in dimension 5, sampling 10^6 frequencies from the Bessel distribution of parameter $s = 2$ on \mathbb{N}^5 yields only $\approx 10^4$ unique frequencies. This allows for tighter certificates, as it makes the r.h.s of eq. (9), in $1/N$, much smaller. Note that the time to generate this hash table is *not* reported in tables 1 and 2 and of the order of a few seconds.

D Other computation

Lemma 4. Let f be the function defined on $(-1, 1)$ with

$$\forall u \in (0, 1/2), \quad f(\cos 2\pi u) = e^{s \cos 2\pi(u-v)}. \quad (32)$$

Then, its Chebychev coefficient are given with

$$f_\omega = (1 + \mathbf{1}_{\omega \neq 0}) \cos(2\pi\omega v) I_\omega(s). \quad (33)$$

Proof. The $\omega \in \mathbb{N}_*$. The component ω of a function f on the Chebychev basis is given with

$$f_\omega = \frac{2}{\pi} \int_{-1}^1 f(x) T_\omega(x) \frac{dx}{\sqrt{1-x^2}},$$

which we conveniently rewrite, with the classical change of variable $x = \cos 2\pi u$,

$$f_\omega = 2 \int_{I_1} f(\cos 2\pi u) \cos(2\pi\omega u) du \quad (34)$$

which is valid for any interval $I_1 \subset \mathbb{R}$ of length 1.

Now, for $s > 0$, consider the function f defined on $(-1, 1)$ with $x \mapsto e^{s \cos(\arccos(x) - 2\pi v)}$, or equivalently

$$\forall u \in (0, 1/2), \quad f(\cos 2\pi u) = e^{s \cos 2\pi(u-v)}. \quad (35)$$

Putting eq. (35) into eq. (34), we obtain

$$\begin{aligned} f_\omega &= 2 \int_{I_1} e^{s \cos 2\pi(u-v)} \cos(2\pi\omega u) du \\ &= 2 \int_{I_1} e^{s \cos 2\pi u} \cos(2\pi\omega(u+v)) du \\ &= 2 \int_{I_1} e^{s \cos 2\pi u} \cos(2\pi\omega u) \cos(2\pi\omega v) du - 2 \int_{I_1} e^{s \cos 2\pi u} \sin(2\pi\omega u) \sin(2\pi\omega v) du. \end{aligned}$$

490 The last term is odd, hence integrate to 0 on an interval centered around 0. Hence,

$$f_\omega = 2 \cos(2\pi\omega v) \int_{I_1} e^{s \cos 2\pi u} \cos(2\pi\omega u) du. \quad (36)$$

491 We recognize the definition of the modified Bessel function of the first kind, defined in eq. (14).
492 Plugging this into eq. (36), we obtain

$$f_\omega = 2 \cos(2\pi\omega v) I_\omega(s) = 2 I_\omega(s) H_\omega(\cos(2\pi v)). \quad (37)$$

493 If $\omega = 0$, we add a factor $1/2$ into the definition in eq. (34), which yields

$$f_\omega = I_0(s). \quad (38)$$

494

□

495 References

- 496 [1] Pablo Moscato et al. On evolution, search, optimization, genetic algorithms and martial
497 arts: Towards memetic algorithms. *Caltech concurrent computation program, C3P Report*,
498 826(1989):37, 1989.
- 499 [2] Reiner Horst and Panos M Pardalos. *Handbook of global optimization*, volume 2. Springer
500 Science & Business Media, 2013.
- 501 [3] Stephen P Boyd and Lieven Vandenbergh. *Convex optimization*. Cambridge university press,
502 2004.
- 503 [4] Peter JM Van Laarhoven, Emile HL Aarts, Peter JM van Laarhoven, and Emile HL Aarts.
504 *Simulated annealing*. Springer, 1987.
- 505 [5] Jean Bernard Lasserre. *Moments, Positive Polynomials and Their Applications*, volume 1 of
506 *Series on Optimization and Its Applications*. IMPERIAL COLLEGE PRESS, October 2009.
- 507 [6] Jean B. Lasserre. Global Optimization with Polynomials and the Problem of Moments. *SIAM*
508 *Journal on Optimization*, 11(3):796–817, January 2001.
- 509 [7] Blake Woodworth, Francis Bach, and Alessandro Rudi. Non-Convex Optimization with Cer-
510 tificates and Fast Rates Through Kernel Sums of Squares. In *Proceedings of Thirty Fifth*
511 *Conference on Learning Theory*, pages 4620–4642. PMLR, June 2022.
- 512 [8] Ian Goodfellow, Yoshua Bengio, and Aaron Courville. *Deep learning*. MIT press, 2016.
- 513 [9] Didier Henrion, Milan Korda, and Jean-Bernard Lasserre. *The Moment-SOS Hierarchy*, vol-
514 ume 4 of *Optimization and Its Applications*. World Scientific Publishing Europe Ltd., December
515 2020.
- 516 [10] Hayato Waki, Sunyoung Kim, Masakazu Kojima, and Masakazu Muramatsu. Sums of Squares
517 and Semidefinite Program Relaxations for Polynomial Optimization Problems with Structured
518 Sparsity. *SIAM Journal on Optimization*, 17(1):218–242, January 2006.
- 519 [11] Jie Wang, Victor Magron, and Jean-Bernard Lasserre. TSSOS: A Moment-SOS Hierarchy That
520 Exploits Term Sparsity. *SIAM Journal on Optimization*, 31(1):30–58, January 2021.
- 521 [12] Jie Wang, Victor Magron, and Jean-Bernard Lasserre. Chordal-TSSOS: A Moment-SOS
522 Hierarchy That Exploits Term Sparsity with Chordal Extension. *SIAM Journal on Optimization*,
523 31(1):114–141, January 2021.
- 524 [13] Francis Bach and Alessandro Rudi. Exponential convergence of sum-of-squares hierarchies for
525 trigonometric polynomials, January 2023.
- 526 [14] Monique Laurent and Lucas Slot. An effective version of schmüdgen’s positivstellensatz for the
527 hypercube. *Optimization Letters*, September 2022. Funding Information: This work is supported
528 by the European Union’s Framework Programme for Research and Innovation Horizon 2020
529 under the Marie Skłodowska-Curie Actions Grant Agreement No. 764759 (MINOA). Publisher
530 Copyright: © 2022, The Author(s).

- 531 [15] Ngoc Hoang Anh Mai, J. B. Lasserre, Victor Magron, and Jie Wang. Exploiting Constant
532 Trace Property in Large-scale Polynomial Optimization. *ACM Transactions on Mathematical*
533 *Software*, 48(4):40:1–40:39, December 2022.
- 534 [16] Ulysse Marteau-Ferey, Francis Bach, and Alessandro Rudi. Non-parametric Models for Non-
535 negative Functions. In H. Larochelle, M. Ranzato, R. Hadsell, M. F. Balcan, and H. Lin, editors,
536 *Advances in Neural Information Processing Systems*, volume 33, pages 12816–12826. Curran
537 Associates, Inc., 2020.
- 538 [17] Eloïse Berthier, Justin Carpentier, Alessandro Rudi, and Francis Bach. Infinite-Dimensional
539 Sums-of-Squares for Optimal Control. In *2022 IEEE 61st Conference on Decision and Control*
540 *(CDC)*, pages 577–582, December 2022.
- 541 [18] Boris Muzellec, Adrien Vacher, Francis Bach, François-Xavier Vialard, and Alessandro Rudi.
542 Near-optimal estimation of smooth transport maps with kernel sums-of-squares, December
543 2021.
- 544 [19] Alessandro Rudi and Carlo Ciliberto. PSD Representations for Effective Probability Models. In
545 *Advances in Neural Information Processing Systems*, volume 34, pages 19411–19422. Curran
546 Associates, Inc., 2021.
- 547 [20] Alessandro Rudi, Ulysse Marteau-Ferey, and Francis Bach. Finding Global Minima via Kernel
548 Approximations. *arXiv:2012.11978 [cs, math, stat]*, December 2020.
- 549 [21] Pascal Van Hentenryck. Machine Learning for Optimal Power Flows. *INFORMS Tutorials in*
550 *Operations Research*, October 18.
- 551 [22] Joseph J. Hilling and Anthony Sudbery. The geometric measure of multipartite entanglement
552 and the singular values of a hypermatrix. *Journal of Mathematical Physics*, 51(7):072102, July
553 2010.
- 554 [23] Irène Waldspurger, Alexandre d’Aspremont, and Stéphane Mallat. Phase Recovery, MaxCut
555 and Complex Semidefinite Programming, July 2013.
- 556 [24] Ingo Steinwart and Andreas Christmann. *Support vector machines*. Springer Science & Business
557 Media, 2008.
- 558 [25] The Basic Theorems of Fourier Analysis. In *Fourier Analysis on Groups*, chapter 1, pages 1–34.
559 John Wiley & Sons, Ltd, 1990.
- 560 [26] Luc Devroye, Matthieu Lerasle, Gabor Lugosi, and Roberto I. Oliveira. Sub-Gaussian Mean
561 Estimators. *The Annals of Statistics*, 44(6):2695–2725, 2016.
- 562 [27] G. N. Watson. *A Treatise on the Theory of Bessel Functions*. Cambridge University Press, 1922.
- 563 [28] Vern I. Paulsen and Mrinal Raghupathi. *An Introduction to the Theory of Reproducing Kernel*
564 *Hilbert Spaces*. Cambridge Studies in Advanced Mathematics. Cambridge University Press,
565 Cambridge, 2016.
- 566 [29] Jie Wang and Victor Magron. Exploiting Sparsity in Complex Polynomial Optimization. *Journal*
567 *of Optimization Theory and Applications*, 192(1):335–359, January 2022.
- 568 [30] Cédric Josz and Daniel K. Molzahn. Lasserre Hierarchy for Large Scale Polynomial Optimiza-
569 tion in Real and Complex Variables. *SIAM Journal on Optimization*, 28(2):1017–1048, January
570 2018.